CROSS-SECTIONAL GRADIENTS OF RESIDUAL STRESSES, MICROSTRUCTURE AND PHASES IN A NITRIDED STEEL REVEALED BY 20µm SYNCHROTRON X-RAY DIFFRACTION

S. C. Bodner, T. Ziegelwanger, M. Meindlhumer, J. Holcova, J. Todt, N. Schell, J. Keckes

Cross-sectional gradients of residual stresses, phases, microstructure, composition and mechanical properties within the near-surface regions of thermo-chemical treated steels are decisive for the balanced mechanical properties of the final products. In this work, a correlative cross-sectional micro-analytics is introduced to assess those gradients in an exemplary nitrided steel sample to a depth of ~0.8 mm. Cross-sectional synchrotron X-ray microdiffraction with an energy of 87.1 keV and a spatial resolution of 20 µm was performed in transmission diffraction geometry. At first, a methodology to evaluate residual stress magnitudes from two-dimensional X-ray diffraction data is discussed. The data from a ~2.5 mm long sample gauge volume indicate complex residual stresses and near-surface microstructure gradients with a maximal compressive stress of ~-400 MPa, descending diffraction peak broadening and variable crystallographic texture. The results correlate well with the complementary analyses of Vickers micro hardness and sample cross-sectional morphology. In summary, the correlative cross-sectional micro-analytics documents the possibility to determine and correlate a variety of mechanical, structural, morphological and chemical sample parameters obtained using cutting-edge characterization approaches. The complex experimental data can be further used to adjust and verify numerical and technological models.

KEYWORDS: SYNCHORTRON MICRO X-RAY DIFFRACTION - CROSS-SECTIONAL CHARACTERIZATION - NITRIDING – RESIDUAL STRESSES.

INTRODUCTION

Thermochemical treatments like nitriding, nitrocarburizing or carburizing have been well known to in-crease the performance of engineering steel components. The reason for the enhancement of wear re-sistance, mechanical strength and fatigue behavior are gradients in the near surface regions up to a depth of a few hundreds of micrometers. In order to further improve the functional properties of the steels, however, it is necessary to optimize the thermochemical treatments technology, which go hand in hand with the understanding of the processes taking place during the surface treatment at micro and nano scale. Consequently, there is a need to design novel characterization techniques and strategies that can expound the impact of particular processing strategies on material's functional properties.

In this contribution, a correlative cross-sectional micro-analytics is introduced to analyze mechanical, structural, morphological and chemical properties of an exemplary nitrided low alloy steel sample. Primari-ly, a focused high energy X-ray beam with a width of ~20 µm is used to scan a cross-section of the sam-ple in order to assess the complex depth gradients of phases, microstructure and residual stresses (1). Additionally optical microscopy and micro-hardness profiling were used to obtain complementary data from the sample.

S. C. Bodner, T. Ziegelwanger, M. Meindlhumer, J. Holcova, J. Keckes
Department of Materials Science, Institute of Materials Physics, Montanuniversität Leoben, Austria

J. Todt
Erich Schmid Institute for Materials Science, Austrian Academy of Science, Austria

N. Schell
Institute of Materials Research, Helmholtz-Zentrum Geesthacht, Germany

EXPERIMENTAL PROCEDURE

Sample Preparation

A disc-shaped, gas nitrided cylinder with a diameter of 40 mm and a thickness of 10 mm was exemplarily characterized in this work. The base material is a low alloy steel with a carbon content of less than 0.2%, typically used for case hardening in a pre-heat treaded state and provided in an industrial standard grade.

Characterization Techniques

To prepare the sample for the synchrotron transmission diffraction experiment, (cf. Fig. 1), a platelet of ~2.5 mm in thickness was extracted from the sample by precision cutting at a Accutom-5 system (Struers, Germany), equipped with a diamond cutting wheel.

The sample cross-section was scanned in transmission at the HEMS beamline P07 at the storage ring PETRA III in Hamburg, Germany (2) using a beam energy of 87.1 keV. Fig. 1 provides a schematic representation of the experimental setup, which will be further denoted as cross-sectional X-ray microdiffraction (CSmicroXRD). The rectangular beam cross-section was ~(500 x 20) µm² corresponding to the beam width and the height (Fig. 1). The scanning increment was set to 20 µm. A two-dimensional (2D) amorphous silicon digital X ray detector (model XRD1621 by PerkinElmer) with a pixel pitch of ~200 µm collected the diffraction signals. LaB6 standard was used to determine the sample-to-detector distance of 1329 mm.

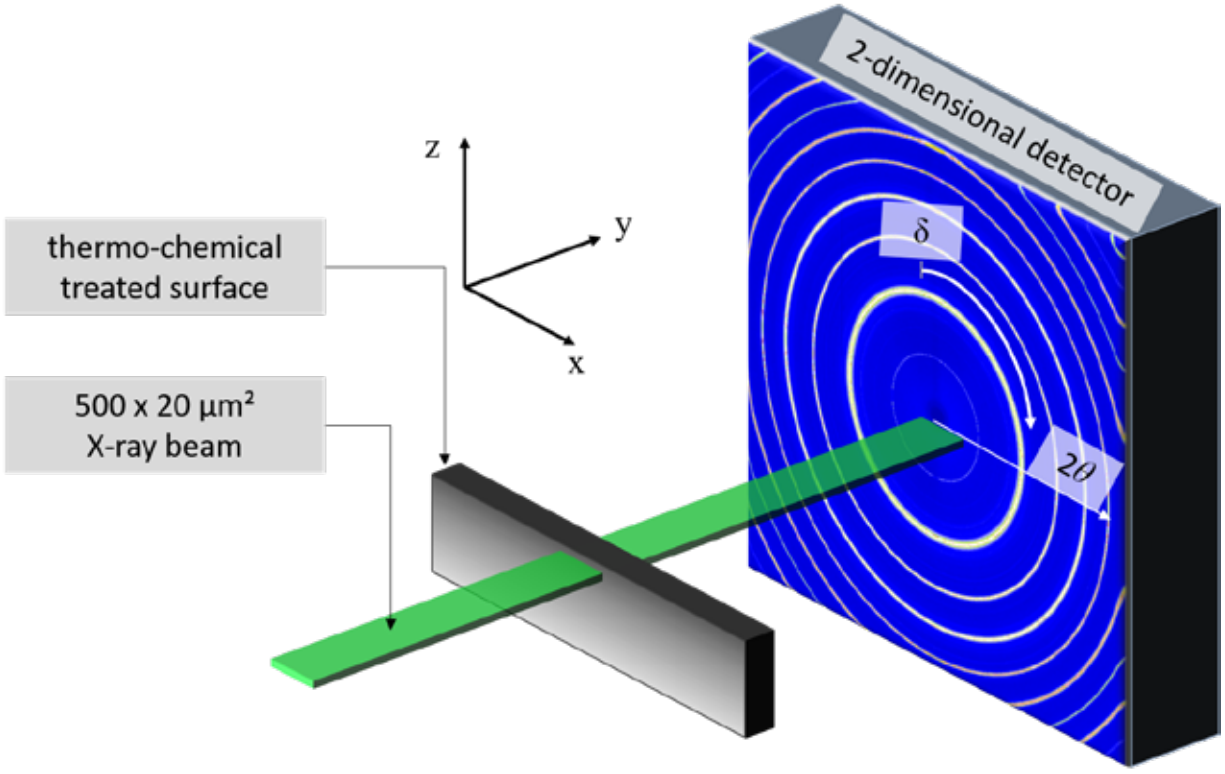

Fig. 1 - Experimental setup of the CSmicroXRD experiment at DESY in Hamburg. The cross-section of the thermo-chemical treated sample is being scanned in transmission diffraction geometry by moving the sample in the beam along the z-axis with an increment of ~20 µm. At each scanning position, two-dimensional X-ray diffraction data are collected using a 2D detector.

The microstructure of the sample was studied by optical microscopy from the metallurgical cross sections. Therefore, the specimen was hot-embedded at 180°C at a pressure of 15 kN for 900 seconds before it was grinded, polished and etched with a Nital 3% etchant.

Vicker's hardness profiles were determined on the embedded sample using a Mitutoyo/Buehler Micromet 5104 testing device. A testing force of 4.90 N – corresponding to HV0.5 – was used to indent the polished, unetched cross-section. The hardness values given in Fig. 2c were calculated by averaging the result of multiple indents at redundant depth positions.

METHODOLOGICAL APPROACH

Debye-Scherrer rings collected using the 2D detector contains information on the lattice parameters, crystallographic texture, crystallite size and strain state of phases within the gauge volume. The 2D data were analyzed using a Python pyFAI software package (3).
An integration of the 2D diffraction data over the azimuthal angle δ (Fig. 1) was used to obtain an intensity distribution as a function the Bragg's angle θ and the obtained I(θ) data were used for the determination of the lattice parameters and the identification of the particular crystalline phases in the sample.
Crystallographic texture was determined by analyzing the azimuthal intensity distributions of the Debye-Scherrer rings of the martensite phase in an angular range of $0 < \delta < 90°$.

An information on the size of the coherently scattering domains and strains of II and III order can be obtained by analyzing the full width at half maximum (FWHM) of the diffraction peaks. Since FWHM data can be derived as a function of the azimuthal angle δ, FWHM analysis can be used to obtain direction dependent microstructural properties of the sample (4).

Residual strain depth gradients along the scanning direction z (Fig. 1) can be determined by the evalua-tion of the Debye-Scherrer ring's ellipticity. In general, X-ray elastic strain along the diffraction vector specified by the angles δ and θ (7) can be expressed as follows (5)

$$\varepsilon(\delta,\theta) = \frac{d(\delta,\theta) - d_0}{d_0}$$

[1]

where d_0 is the unstrained lattice parameter and d(δ,θ) is the direction dependent lattice parameter.

Since the initial geometry of the sample was rotationally symmetric, it can be approximated that there was no significant in-plane sample anisotropy and for the in-plane strain components ε_{11} (z)=ε_{22} (z) is valid. Furthermore, it was for simplicity supposed that the shear strain and stress components can be neglected with $\varepsilon_{ij} \cong 0$ and $\sigma_{ij} \cong 0$. Consequently, the measured in-plane X-ray elastic strain ε(δ,θ) can be expressed as

$$\varepsilon(\delta,\theta) = sin^2\theta\ \varepsilon_{11} + cos^2\theta\ sin^2\delta\varepsilon_{11} + \varepsilon_{33}\ cos^2\delta,$$

[2]

where ε_{ii} represents the unknown sample depth-dependent X-ray elastic strain components, while the indices i = 1,2 and 3 correspond to the axis x, y and z in Fig. 1.
As extensively discussed in reference (6), by inserting the X-ray elastic constants S_1 (hkl) and ½ S_2 (hkl) in Eq. 2 and considering the relationship between X-ray elastic strains and unknown stresses σ_{ii}, the distortion of the Debye-Scherrer rings as a function of the sample's depth z can be expressed as

$$\frac{\partial d(\delta,z)}{\partial sin^2\delta} = \sigma_{22}(z)\frac{1}{2}S_2\ d_0(z)$$

[3]

where σ_{22} (z) represents to the magnitude of depth dependent in-plane residual stresses.
In contrast to the cross-sectional X-ray nanodiffraction analysis (CSnanoXRD) described in (1,6–8), the out-of-plane residual stress component σ_{33} (z) cannot be always considered to be negligible at sample depths of several hundreds microns. Consequently, in the case of CSmicroXRD, Eq. 3 must be modified as follows

$$\frac{\partial d(\delta,z)}{\partial sin^2\delta} = (\sigma_{22}(z) - \sigma_{33}(z))\ \frac{1}{2}S_2\ d_0(z)$$

[4]

RESULTS AND DISCUSSION

Experimental data obtained using the correlative cross-sectional micro-analytics, including CSmicroXRD, microscopy and hardness profile characterization, are presented in Fig. 2. Due to the insufficient detector resolution, reflections of the martensite and the bainite coincide and appear as one in depth-resolved phase plot of the nitrided sample in Fig. 2a. Therefore, the bainite reflections notation was used. The peaks of the thin compound layer directly at the sample's surface are clearly visible in the colored illustration which is provided in the electronic version of the ECHT2019 conference proceedings. They indicate the presence of ε nitrides. The spatial resolution could be improved by choosing a smaller X-ray beam size and a scanning increment in the near-surface region. Fig. 2b shows the azimuthal intensity distribution of the α110 peak. The quantitative analysis of the texture gradient within the sample indicates a presence of random texture in the near-surface region and emerging texture at depths of ~280 µm and more.

Results from Vicker's hardness measurements are presented in Fig. 2c. The values decrease within ~250 µm from 514 $HV_{0.5}$ at a depth position of ~50 µm to the core hardness of 232 $HV_{0.5}$. An effective nitriding depth of ~180 µm was determined. The optical micrograph displays zones within different microstructure. The surface is covered by a ~4 µm thin, continuously formed compound layer after which the nitrogen diffusion zone is present up to a depth of ~90 µm. The thickness of the compound layer and the diffusion zone was identified by optical microscopy with ~4 and ~90 µm, respectively. Adjacently, a region richer on carbides in a bainitic matrix follows due to the displacement and rearrangement of interstitial carbon by nitrogen in the diffusion zone. The optical micrograph shows, that the microstructure changes again at the total nitring depth of ~280 µm below the surface to the bainitic core material.

Fig. 2d and Fig. 2e show the αb 200 peak in in-plane and out-of-plane diffraction vector orientation, respectively. In the case of in-plane orientation, a peak shift to higher Bragg angles in the reciprocal space corresponds to a compression of the crystal planes and negative strain in the real space. In other words, the peak shift to higher Bragg angles indicate the presence of in-plane compressive stresses. This correlates with the peak shift to smaller Bragg angles in Fig. 2e, indicating lattice parameter increase and positive strains, for out-of-plane diffraction vector orientation. The lattice parameter increase in Fig. 2e observed within the first ~90 µm below the surface is caused by the same compressive in-plane residual stress that are formed by the nitriding process.

In the next step, stresses were evaluated from the αb 211 peak by applying X-ray elastic constants. As indicated by the peak shifts (cf. Figs. 2d,e), the analysis of the data revealed a compressive stress profile along the sample's depth. The stress maximum of ~-415 MPa was determined ~20 µm below the surface. More than 60% of the stress relaxation takes place, however, within the diffusion zone of the sample. The slope of the relaxation changes and the remaining stress reliefs within the following 160 µm and stays approximately constant after.

In summary, correlative cross-sectional micro-analytics and CSmicroXRD represent powerful tools to resolve depth gradients of phases, texture, residual stresses, microstructure and mechanical properties across gradient materials such as nitrided, carburized, quenched and tempered steels. In comparison to standard techniques used to characterize the residual stress state in gradient steels, CSmicroXRD offers the possibility of a rapid scanning of the specimens - after the sample alignment, all experimental data from Figs. 2a,b,d-f were captured within ~250 seconds. A further advantage is the simple sample preparation, even industrial parts with a complex geometry can be characterized position resolved as one-part without cuttig by applying the conical slit system (9). Finally, the experimental data obtained using cross-sectional micro-analytics and CSmicroXRD (Fig. 2) can be used to verify numerical and technological models as well as applied to further predict the effect of modified and adapted thermochemical treatments.

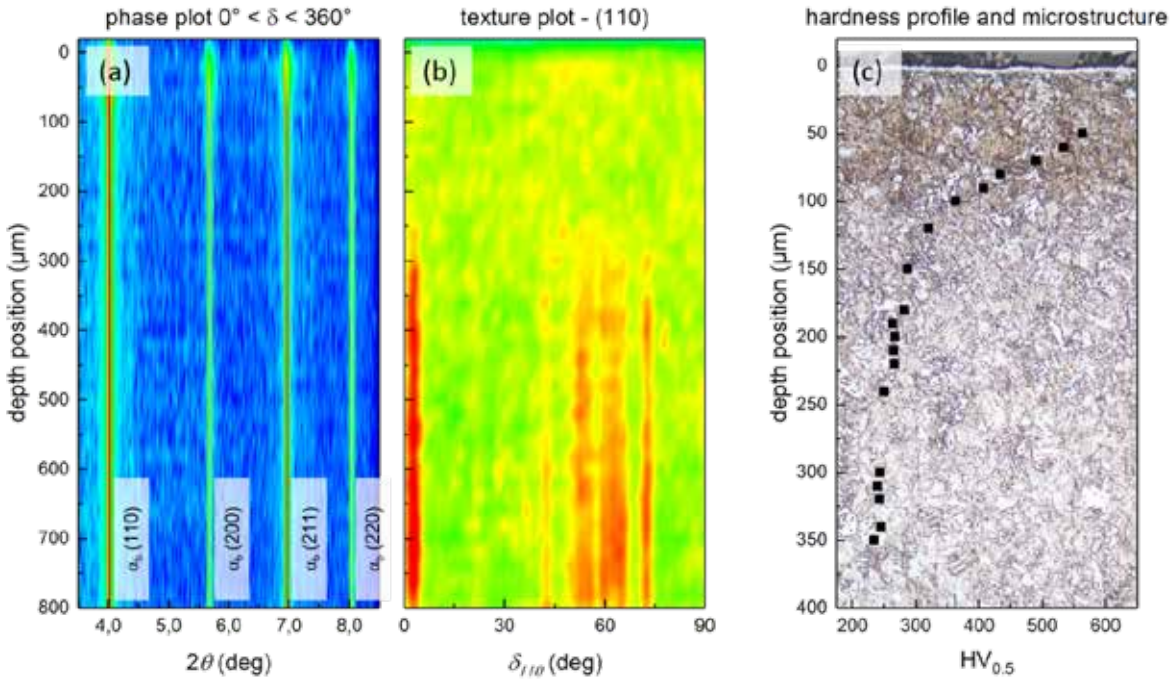

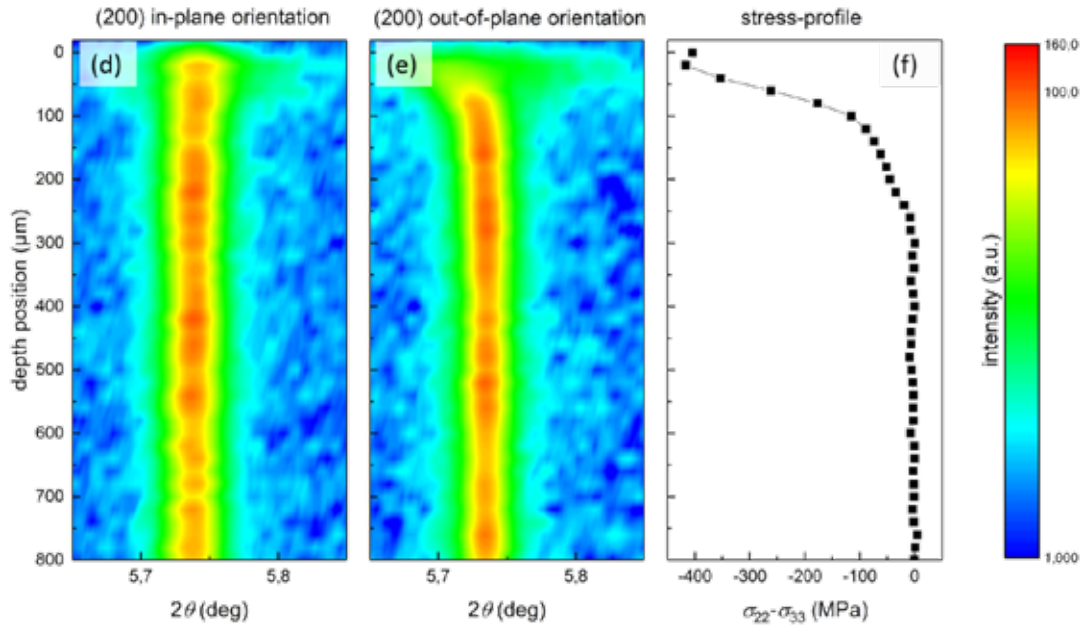

Fig. 2 - Depth-resolved experimental results from the gas nitrided martensitic steel sample. (a) Phase plot with the particular reflections. (b) The quantitative texture analysis indicates random near-surface texture induced by the thermo-chemical heat treatment. (c) Hardness values decrease gradually within the diffusion zone of the layer and are slightly elevated down to a depth of ~230 µm (carbide-rich zone). (d,e) Zooms to the in-plane and out-of-plane orientations of the 200 peak show the shift to higher and lower angles, respectively, due to in-plane residual compressive stresses. (f) The depth resolved stress profile indicates a maximum at ~20 µm after which the stress relaxes in two steps with different relaxation slopes.

REFERENCES

[1] Kurz SJB, Meka SR, Schell N, Ecker W, Keckes J, Mittemeijer EJ. Residual stress and microstructure depth gradients in nitrided iron-based alloys revealed by dynamical cross-sectional transmission X-ray microdiffraction. Acta Materialia [Internet]. Acta Materialia Inc.; 2015;87:100–10. Available from: http://dx.doi.org/10.1016/j.actamat.2014.12.048

[2] Schell N, King A, Beckmann F, Ruhnau HU, Kirchhof R, Kiehn R, et al. The High Energy Materials Science Beamline (HEMS) at PETRA III. In: AIP Conference Proceedings. 2010.

[3] Kieffer J, Karkoulis D. PyFAI, a versatile library for azimuthal regrouping. In: Journal of Physics: Conference Series. 2013.

[4] Scherrer P. Bestimmung der Größe und der inneren Struktur von Kolloidteilchen mittels Röntgenstrahlen. Nachrichten von der Gesellschaft der Wissenschaften zu Göttingen, Mathematisch-Physikalische Klasse. 1918;

[5] Dölle H. The influence of multiaxial stress states, stress gradients and elastic anisotropy on the evaluation of (Residual) stresses by X-rays. journal of Applied Crystallography. 1979;

[6] Stefenelli M, Todt J, Riedl A, Ecker W, Müller T, Daniel R, et al. X-ray analysis of residual stress gradients in TiN coatings by a Laplace space approach and cross-sectional nanodiffraction: A critical comparison. Journal of Applied Crystallography. 2013;46(5):1378–85.

[7] Keckes J, Bartosik M, Daniel R, Mitterer C, Maier G, Ecker W, et al. X-ray nanodiffraction reveals strain and microstructure evolution in nanocrystalline thin films. Scripta Materialia. 2012;

[8] Bartosik M, Daniel R, Mitterer C, Matko I, Burghammer M, Mayrhofer PH, et al. Cross-sectional X-ray nanobeam diffraction analysis of a compositionally graded CrN x thin fi lm. 2013;542:1–4.

[9] Staron P, Fischer T, Eims EH, Frömbgen S, Schell N, Daneshpour S, et al. Depth-Resolved Residual Stress Analysis with Conical Slits for High-Energy X-Rays. Materials Science Forum. 2013;